

SKD: Unsupervised Keypoint Detection for Point Clouds using Saliency Estimation

Georgi Tinchev, Adrian Penate-Sanchez, and Maurice Fallon

University of Oxford, United Kingdom
{gtinchev,adrian,mfallon}@robots.ox.ac.uk

Abstract. In this work we present a novel keypoint detector that uses saliency to determine the best candidates from point clouds for tasks such as registration and reconstruction. The approach can be applied to any differentiable deep learning descriptor by using the gradients of that descriptor with respect to the input to estimate an initial set of candidate keypoints. By using a neural network over the set of candidates we can also learn to refine the point selection until the actual keypoints are obtained. The key intuition behind this approach is that keypoints need to be determined based on how the descriptor behaves given a task and not just because of the geometry that surrounds a point. To improve the performance of the learned keypoint descriptor we combine the saliency, the feature signal and geometric information from the point cloud to allow the network to select good keypoint candidates. The approach was evaluated on two large LIDAR datasets - the Oxford RobotCar dataset and the KITTI datasets, where we obtain up to 50% improvement over the state-of-the-art in both matchability score and repeatability. This results in a higher inlier ratio and a faster registration without compromising metric accuracy.

Keywords: Unsupervised keypoint detection, registration, point cloud

1 Introduction

A key task for localization and reconstruction is the repeatable extraction of points that can be reliably matched with a map or another representation of the same environment or object. Image keypoint extraction has been well studied, but point cloud keypoint extraction is less explored. In this work, we present a novel method for keypoint extraction from point clouds that exploits the spatial information encoded within each feature to suggest points with higher likelihood of being matched which improves the performance of the *keypoint and feature* pair.

Traditionally, keypoint extraction methods have only focused on the local geometry of the image, such as the Harris corner detector [9] or the more efficient Difference-of-Gaussians approach which is used in SIFT [16]. These methods focused on understanding the geometry of the image so as to match points present in a pair of images, known as *repeatability*. If corresponding points are obtained

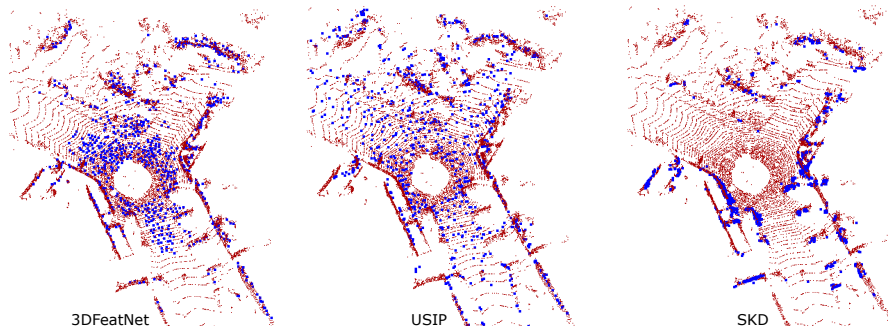


Fig. 1. Top down view of a single point cloud (brown) and 1024 generated keypoints (blue). Our method (SKD) was not implicitly trained to ignore the ground, but rather uses the feature signal of the descriptor and the context information to determine informative areas in the environment - corners, edges and structure.

from two different images of the same scene, one can then find matches between them without introducing incorrect matches (outliers). If the outlier percentage is low, a robust estimator [6] can converge faster and produce a better solution. The problem with this approach is that it ignores how the feature will react to disturbances. The fact that a point is in the same physical place does not mean that the descriptor will produce the same response. Therefore, one has to look at the combination of *keypoint and feature* performance — namely *matchability*. As evident by recent research [4], repeatability is not sufficient for evaluating keypoint quality. The only reliable metric is matchability, as it measures how useful the combination of *keypoint and feature* is. For this reason we focus here on building a keypoint detector that learns to produce points that can be reliably matched given a deep learning descriptor. All our experiments are based on the state-of-the-art feature descriptor for point cloud data — 3DFeatNet [35]. We use the gradient response of the descriptor with respect to the input point cloud and combine it with contextual information from the point cloud in order to produce keypoints that generate a higher percentage of inlier matches.

The proposed approach leverages the idea, presented in [4], that state-of-the-art keypoint detectors can be built by using only the feature gradients with respect to the input. The gradients encode much of the local information used by the feature descriptor. The points of maximum gradient response provide a set of very promising candidate points. Using this initial set of keypoints, we enforce the notion of *saliency* that uses the combination of neural network layer activations and the gradients at that layer w.r.t. the input to select more characteristic keypoints (Fig. 1). The use of saliency has been shown to produce promising results both in images and in point clouds [28,29,39]. This subset of the original points will then be combined within a neural network that looks at the geometry of the point cloud and makes a decision as to which are the best points to select. The main contributions of our work are as follow:

- Unsupervised learning of keypoints: similar to [13], we require only the rotation and translation between two point clouds when learning to predict reliable keypoints from a point cloud.
- A context agnostic approach: by combining the gradient response with the semantic information of a point cloud, our approach is less vulnerable to biases in the training data. This makes our approach robust when testing on a different context and allows the model to be used without retraining. We demonstrate this by training on the Oxford RobotCar dataset [18] and testing on the KITTI dataset [7] without retraining.
- State-of-the-art performance: Compared to the state-of-the-art [35,13], our approach generates two times more correct matches and achieves 40% more relative repeatability. We have evaluated our algorithm on the two largest and most widely used LIDAR datasets - the Oxford RobotCar dataset [18] and the KITTI dataset [7]. In total these datasets contain point clouds collected from more than 300 kilometers of experiments.

2 Related Work

This paper focuses on reliably obtaining keypoints from point clouds. This is a topic which is very closely related to image keypoint extraction, so we will review the literature for both fields in this section. We will also outline the relevant work that has been done on point cloud-based deep learning models and saliency methods as these topics are central to the contributions of our approach.

2.1 Image Keypoint Detectors

Much of the recent work on keypoint and feature extraction from images employs deep learning architectures. In [8] a keypoint detector for depth images is presented. It uses a Siamese approach by pairing two Faster-RCNN networks [24] and then enforcing a contrastive loss. Quad-Networks [25] developed an unsupervised keypoint generator by learning to rank points and keeping this rank before and after transformation while looking at the top and bottom quartiles. Methods such as [10] and [38] extract unsupervised landmarks. They find the best possible cues to improve the performance of a given task.

Approaching landmark generation in an unsupervised fashion is the equivalent to learning keypoints, because no ground-truth points exist, the regions that maximize the end-task performance must be manually selected. Specific to unsupervised keypoint learning, [12] presents an approach that generates reliable keypoints by learning from the temporal consistency of the network activations in short videos. A successful approach to obtain good keypoints is to optimize how they respond to the content of the image and not just the geometry. TILDE [31] learns to make the points more reliable by understanding how changes in weather and lighting modify the performance of a point. An important distinction is that

this no longer focuses solely on keypoints with reliable geometry, but also looks at the content and the context of the point.

In LIFT [36], the keypoint detector and the feature descriptor are jointly learned by leveraging structure from motion sequences to generate great amounts of training data. By understanding that the job of a keypoint is to increase the probability of a descriptor matching, LIFT focused on matching performance and at the time outperformed all previous approaches. Very recently, ELF [4] applied a simple approach by using the gradient response of deep learning features to produce keypoints. They managed to outperform both TILDE and LIFT without needing to train. Their approach obtains very reliable embedding information by looking at the feature activations.

2.2 Point Cloud Keypoint Detectors

A series of approaches build upon PointNet [22] and PointNet++ [23] introduced new ways to efficiently understanding unstructured sets of points (point clouds). By learning a symmetry function approximated by a multi-layer perceptron (MLP) the authors proposed a new kind of layer that could learn an approximation of a convolutional operator over sets of unordered points. Similarly, [14] managed to increase the performance of the basic neurons by also approximating a convolution using a MLP and by performing aggregation of spatial data within each neuron. [30] presented a method to perform place recognition from point clouds. The point clouds were described using a combination of networks trained with a metric learning loss to produce a feature vector.

Due to the success of the aforementioned approaches, many novel methods leveraged PointNet layers in their work [33,39,20,15,37,5,34,21,32,17]. Recently, in [33], the authors studied how adversarial attacks could affect the performance of the PointNet layers. It also studied how introducing or removing points affected performance. In [39] the authors built a saliency map to understand the effect of each point on the final prediction. They tested the performance of their saliency score by performing point dropping operations to demonstrate performance better than a method based on the critical-subset theory. Frustum PointNets [21] use PointNet layers as the building blocks for their approach and apply it to object detection in point clouds. Their approach produced good quality performance by combining image inputs with point cloud inputs. Also combining images and point clouds for 3D object detection, PointFusion [34] presents a method that focused on bounding box prediction by proposing a novel dense fusion architecture.

The most relevant methods to our work are 3DFeatNet [35] and USIP [13]. 3DFeatNet [35] is the state-of-the-art in feature extraction for point clouds. It uses PointNet++ as a building block and learned a detector and a descriptor by using a two stage network. The main problem with this approach is that the keypoint extraction network does not perform as well as desired. Therefore, recently a novel keypoint extraction method was proposed, USIP [13]. It focused on obtaining keypoints with a high level of repeatability. This increases the performance of the USIP detector compared to the 3DFeatNet detector significantly.

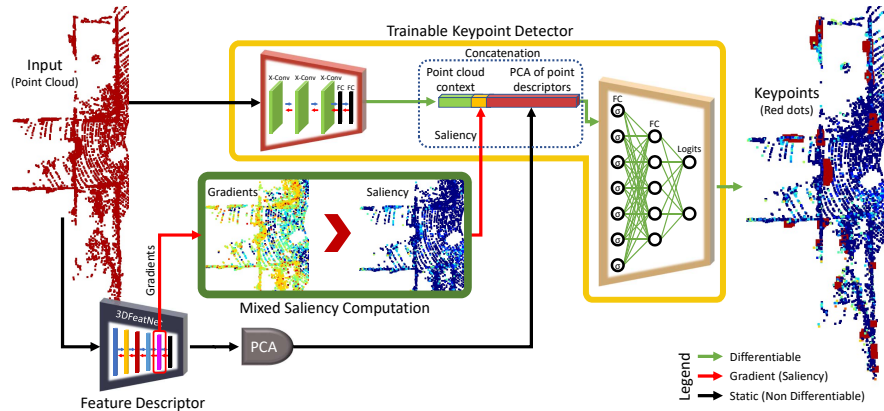


Fig. 2. Proposed network architecture. The input to our system is a raw point cloud and a feature descriptor network. Our method concatenates the *saliency* information from the gradients of the feature descriptor with the per-point context features and a PCA projection of the original feature descriptor. The concatenated vector is the input to two FC layers that generate per-point response at the logits layer.

2.3 Saliency Estimation

Saliency has been studied as a way to quantify and understand what is relevant within a neural network. The definition of *saliency* in this context has been studied by a number of works, [28,19,27,2,1] amongst others, that seek to understand why machine learning models behave as they do. Even before the growth in popularity of neural networks, methodologies such as [3] were being designed to understand why classifiers made specific decisions. This became more prevalent with the adoption of deep learning models for most perception tasks. Approaches such as [28,1] seek to understand what a neural network finds relevant by looking at how the gradients of a given prediction behave. The interpretation is that gradients with higher magnitude in specific areas influence predictions. The use of *saliency* has been demonstrated to be capable of generating state-of-the-art keypoint extractors in images. ELF [4] computes the gradient of the feature map given an image then used the Kapur threshold [11] to select keypoints. In a similar fashion, Grad-CAM [26] used the gradient maps of a classification score to produce regions of interest for a given image that can aid tasks like classification, image captioning or visual question answering.

3 Methodology

We present Salient Keypoint Detection (**SKD**) - a method for unsupervised keypoint extraction based on the *saliency* of a point cloud. We define *saliency* as the combination of the feature activation signal at a specific layer of a pre-trained descriptor and the gradients of the same layer with respect to the input point

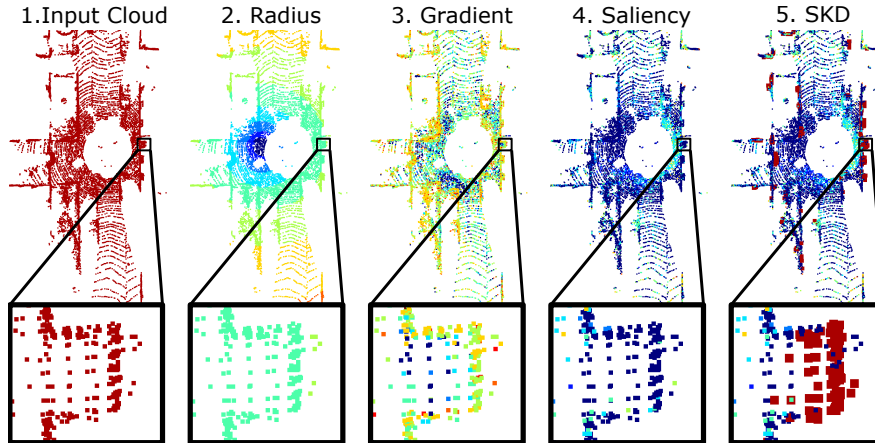


Fig. 3. **1.** Input point cloud P . **2.** Distances of each point (r_i) from the spherical core - blue indicates closer to the median point, red - further apart. **3.** The extracted $S(P)$ signal based on the activations and gradients w.r.t. input point cloud (1.) - blue corresponds to negative gradients, red - highly positive. **4.** The *initial saliency* score s_i estimated from the radius (2.) and the gradients (3.), blue - low score, red - high score. **5.** Selected keypoints (red, enlarged) on top of the saliency score. Our method picks keypoints based on the keypoint saliency score s_i , but also leverages context and the original descriptor to correctly pick out edges and corners negatively scored by s_i .

cloud. We leverage a trained descriptor network to produce robust keypoints directly from 3D data. We then project the *saliency* into the spherical coordinate system of the input point cloud and extract the most informative regions. We combine those regions with *context-aware* features and the features of the original descriptor in order to extract robust and repeatable keypoints. Using the combined feature vector, we train a neural network that learns to predict the likelihood of a point being a keypoint. Similarly to the approach of [4] on images, we extract the gradients of the features at different levels of the architecture, and choose the best performing one. An evaluation of the performance at each layer is presented in Sec. 4.3. In contrast with [4], we select keypoints by combining the gradient information and the activations with the points in Euclidean space in order to determine critical points using the criterion defined by [39].

3.1 Point Cloud Saliency

For a given point cloud $P \in \mathbb{R}^3$, we extract the gradients of a pre-trained network ∇F at a specific layer l with respect to the input, defined as ∇F_l^P . We define the *initial saliency* $S(P)$, as the product of the feature activations of that layer F_l^P with the gradients, formally defined as:

$$S(P) = F_l^P \cdot \nabla F_l^P \quad (1)$$

In this way the extracted initial saliency corresponds to specific points in the point cloud that have good activations and are valuable based on the gradient of that layer w.r.t. the input. From a geometric perspective this can be thought of projecting the feature signal through to the input point cloud, determining the value of individual points. An example projection can be seen in Fig. 3. The initial saliences are of the same dimension as the input point cloud, $S(P) \in \mathbb{R}^3$.

We take these saliences and determine a secondary saliency score per point, defined as s_i for each point $i \in P$. The score weights the contribution of $S(P)$ by the distance from the center of the point cloud in the Spherical Coordinate system. The score is formally defined as:

$$s_i = - \sum_{j=1}^3 [S_j(P) \odot (x_{ij} - \text{median}(x_{ij}))] r_i \quad (2)$$

where $j \in \{1, 2, 3\}$ defines each of the Cartesian coordinates x, y, z of point $i \in P$, \odot is the Hadamard Product and $r_i = \sqrt{\sum_{j=1}^3 (x_{ij} - \text{median}(x_{ij}))^2}$ is the distance of point i to the median of the spherical core of the point cloud [39]. In other words, we transfer the gradient and its activations under the orthogonal coordinates and measure the offset from the center of the point cloud.

This transforms the original point cloud to a spherical coordinate system. Further away points will have higher score, and points closer to the centre will have lower score (see Fig. 3). The reason for doing this is that under any rotation and translation of the input cloud, the centre of the point cloud will not change, and is therefore less informative. Furthermore, when performing geometric registration, selected models (points) that are further apart will provide a more robust solution in comparison to points which are very close together.

Finally, the saliences are normalized to have a zero mean and unit variance within a single point cloud. The final saliency ensures a good spatial distribution of the selected points while also selecting points with good activations based on the descriptor network. Fig. 3 illustrates the saliences of an example input point cloud at each stage of the aforementioned computation.

3.2 Network Architecture

Our network architecture is depicted in Fig. 2. It consists of three parts. The first part is called the *point cloud context* features. This is an ensemble of four X-Conv layers [14] and two fully connected layers that have been pretrained on a feature extraction task to create stable initial estimates. These layers will learn to provide a description of the context around any given point. We use a two dimensional size for the context latent space. The second component is the *saliency* as described in the previous section. The final component is a PCA dimensionality reduction of the original per-point features which improved the final results by producing a smoother feature space. The three components are concatenated and fed to two additional fully connected layers to produce the final keypoint prediction. The network learns to infer a score for each point —

determining the probability of it being a robust and repeatable keypoint for the original descriptor. Note that our model is descriptor-agnostic and thus can be applied to any descriptor network in order to improve the performance. The code for the TensorFlow implementation of our approach will be made available upon publication of the paper.

Training During training, the input to our model consists of a tuple of point clouds and the ground truth transformation between them, namely (P_k, P_l, T) . Both P_k and P_l are $N \times 3$ dimensional vectors, where N denotes the cardinality of the point cloud set. In addition, we assume to have a pre-trained model for the point descriptors. To this end we estimate the saliency s_i and features f_i for each point in both point clouds. Due to the large dimensionality of the feature space f_i , we performed PCA and transformed the features that explained $\approx 90\%$ of the data. This smooths the feature space, which leads to better results.

In addition, given the ground truth transformation between the two point clouds, we determine the bidirectional correspondence for each point, conditioned on the descriptor. These correspondences are used in our loss to select matching pairs of points. Note that these correspondences need not be injective nor surjective. In other words, if for a point i_1 the closest neighbour under the ground truth transformation, T , is j_1 , it does not mean the reverse applies, nor does that limit i_1 to have a unique neighbour from P_l .

For each point in both point clouds we extract what we have called *context-aware features*, f_c , and concatenate them to the saliencies s_i and features f_i . The term *context-aware* is used as we expect the layers that lead to this descriptor to contain information about the local geometry around each point, helping the network to understand the correlations between the local geometry and the point descriptors. We pretrain these layers on a feature learning task to obtain stable initial features in the training. We chose a small feature space of only two dimensions in order to force the network to learn rough estimates of the shape of objects that can generalize better when moving to a different dataset. Afterwards, the full architecture is trained end-to-end with the the saliency and feature concatenation in the middle to create a rich and informative latent space.

The concatenated saliencies, PCA features and *context-aware* features are fed to two fully connected layers to estimate the probability of each of the points being a keypoint. To this end we use a softmax cross entropy loss between the stacked P_k, P_l clouds and the determined correspondences, given the ground truth transformation. Due to the smaller number of correct keypoint correspondences between the two clouds, we balance the loss function terms given the keypoint to non-keypoint ratio determined by the ground truth correspondences.

Inference During the forward pass of the network we estimate a probability of each point being a correct keypoint. We can then either extract the top K keypoints, based on this probability or select all the keypoints based on the probability of each point. The extracted keypoints produced by the described approach are better suited to the descriptor as the learning iterations optimize

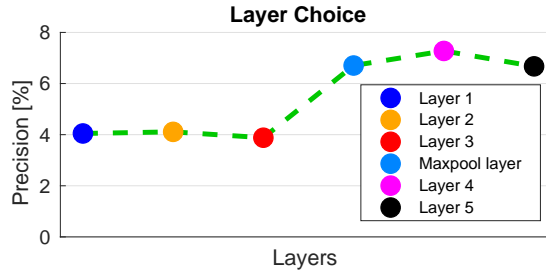


Fig. 4. Evaluation of layers and their performance toward percentage of matches if they were selected for gradient computation. The layer identifier corresponds to the counter of layers in 3DFeatNet [35] starting from the left. For both ELF [4] and our approach we use the layer that maximizes the performance (Layer 4).

its performance. Note, that neither Non-Maximum Suppression, nor any other threshold is applied to obtain the final set of keypoints.

4 Results

In this section we discuss the datasets and metrics we used to evaluate our approach and then present our findings.

4.1 Datasets

In our study we used two datasets - the Oxford RobotCar [18] and the KITTI odometry dataset [7]. In order to provide a fair comparison, our experiments use the preprocessed test data provided by [35] and [13] and we also use their evaluation scripts to make the comparison as fair as possible. We train our model using the same sequences from the RobotCar dataset as [35], and test our approach using the same test set of 3,426 point cloud pairs which the authors provided. Furthermore, we do not train our method nor these baselines on the KITTI dataset, in order to test the generalization ability of the proposed approach.

The evaluation part of the KITTI dataset, used by both [35,13], provides only 2,369 point clouds out of the total dataset. So as to increase the size of the KITTI evaluation dataset, we extended it using the 11 *training* sequences. This is possible only because the RobotCar dataset is used for training all models. The extended dataset is processed in a denser manner: for each point cloud we align the next consecutive 10 point clouds to it using the ground truth transformation. By doing this we expanded the number of testing point cloud pairs from 2,831 to 207,917, which allows us to more fully study our proposed approach.

4.2 Metrics

We used three metrics to compare the performance of our method. We focused our analysis on the keypoint extraction methods. We use the same 3DFeat-

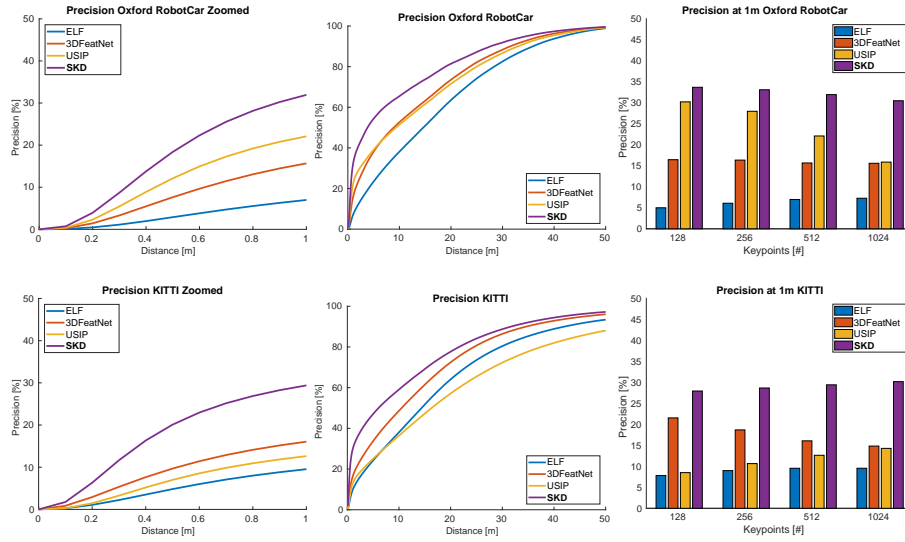


Fig. 5. Matching score evaluated on the Oxford RobotCar dataset (top row) and the KITTI dataset (bottom row). The first two columns are the percentage of matched keypoints using the 3DFeatNet [35] descriptor when varying the distance between correspondences. The first column shows a zoomed-in version of the second column within 1 m of distance, considered relevant for geometric registration. The third column shows the performance of different approaches while varying the number of keypoints.

Net [35] descriptor for all the methods in order to compare the performance of the keypoint detectors.

The first metric uses the matching score as proposed by [35]. We detect keypoints separately for two point clouds. Given the ground truth transformation, we project the keypoints from the first point cloud into the second one. Keypoints that do not have a nearest neighbour in the second point cloud are ignored from the final result (i.e. no overlap). For the rest of the keypoints, the descriptors are compared and matched to establish a correspondence. The precision is measured as the number of correct correspondences against the total number of possible matches. The metric estimates the percentage of correct correspondences based on the distance between them. Correct correspondences are thresholded to 1 m distance, as it serves as a desirable upper limit when performing registration between two point clouds.

For the second metric we chose to compare the normalized relative repeatability, as proposed in [13]. The metric compares the keypoints detected in one point cloud to the keypoints detected in its corresponding point cloud. If the keypoints overlap, below a certain distance, they are considered a match. While this saturates with a high number of keypoints [4], we chose to use the metric to have a fair comparison against USIP [13]. We note that the ability to match

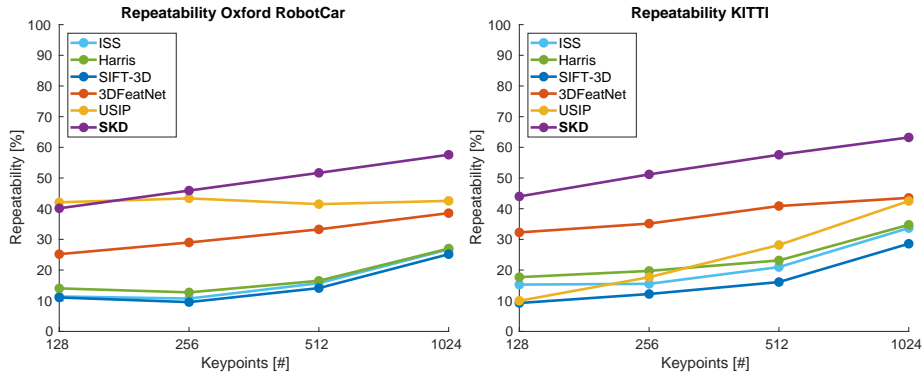


Fig. 6. Quantitative analysis of relative repeatability on the Oxford RobotCar dataset (left) and KITTI (right) measured with different number of extracted keypoints.

keypoints on its own is not sufficient, therefore, we consider the matching score as the more important metric.

Finally, we evaluated the geometric registration of our approach on both the KITTI and the Oxford RobotCar datasets using RANSAC [6]. As in [35], we consider a successful alignment to be all registrations which differ by less than 2 m and 5° from the ground truth transformation. For the successful registrations we present relative translation error (RTE), relative rotation error (RRE), success rate as a percentage of the successful registrations, average number of iterations it took RANSAC to find a suitable candidate within 99% confidence (capped at 10,000 iterations), and the inlier ratio of how many points were considered when obtaining a correct registration.

4.3 Baselines

Our approach is general and can be applied to any point cloud descriptor network. For simplicity we chose to use the descriptor of [35] as it is open source and easy to use, as well as being the state-of-the-art in point cloud point descriptors. We select the best performing layer from the descriptor to generate the gradients on which we compute the saliency values, as evidenced in Fig. 4. We have compared against the learned keypoint detector methods of 3DFeatNet [13] and USIP [35], as well as hand-engineered keypoint extraction methods such as SIFT-3D [16], ISS [40] and Harris-3D [9], and a 3D interpretation of the ELF [4] detector. All the learning methods are trained on the Oxford RobotCar dataset and tested on both RobotCar and KITTI data. We have used the models provided online, and trained our own network. For USIP, we took the models provided by the authors trained on the Oxford RobotCar dataset. As ELF does not need training, we took the best performing layer, in accordance to Fig. 4. We adapt their approach to work on point cloud data by performing Non-Maximum Suppression in 3D and choosing keypoints based on the Kapur Threshold [11].

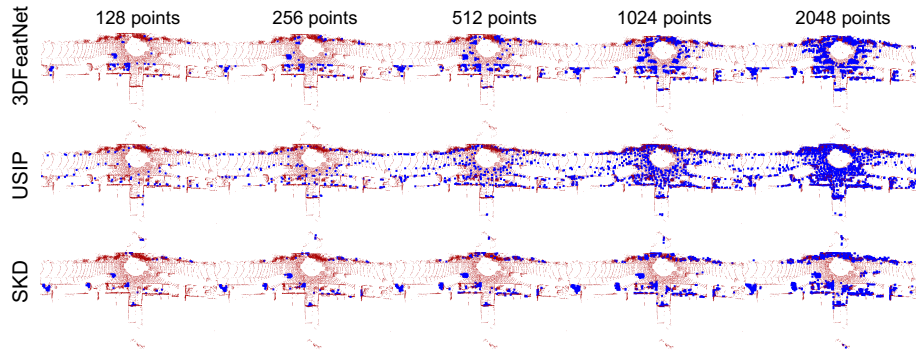


Fig. 7. Qualitative results for the KITTI dataset. For all methods the number of generated keypoints is increased from left to right. This shows what relative importance each method gives to certain areas of the point cloud.

4.4 Matching Score Experiments

Fig. 5 illustrates the performance of SKD compared to other state-of-the-art methods. The first row shows the percentage of matched keypoints on the Oxford RobotCar dataset using the 3DFeatNet descriptor for all methods. The first column is a zoomed-in version of the percentage of points detected within 1 m distance that is considered relevant for matching. The last column shows the precision at 1 m distance at different number of keypoints — 128, 256, 512, 1024. As all the approaches are learning-based, we took the top K keypoints. This ensures that the number of keypoints are identical. The second row presents the results for the full KITTI dataset, with all the methods trained on the Oxford RobotCar dataset. We observe that our approach generalizes well without a loss in performance, and outperforms the second best approach by a significant margin. Also, similarly to 3DFeatNet [35], our approach’s performance does not decline significantly when increasing the number of detected keypoints.

4.5 Repeatability Experiments

Fig. 6 shows the repeatability of SKD measured on the Oxford RobotCar dataset (left) and the KITTI dataset (right). For the Oxford RobotCar, our approach performs comparably to the second best method when extracting 128 and 256 keypoints, but selects points that are 40% more repeatable when extracting 1024 interesting points. Furthermore, Fig. 1 and Fig. 8 present qualitative examples of the detection of keypoints of the top three approaches. The proposed approach has learned to select more descriptive areas of the environment. For example, our method does not select ground points, and even though we forced the method to generate large amounts of points, it still chooses points based on the high activations of the network - around building edges and corners, that in turn are easier to match.

Method	KITTI					Oxford RobotCar	
	RTE (m)	RRE (deg)	Success Rate	Avg # Iter	Inlier rate	Avg # Iter	Inlier rate
3DFeatNet [35]	0.142 ± 0.120	0.533 ± 0.410	97.80%	3917	12.7%	3083	12.9%
USIP [13]	0.203 ± 0.193	0.673 ± 0.517	97.12%	5324	11.0%	823	28.0%
SKD	0.140 ± 0.134	0.579 ± 0.480	96.52%	594	32.2%	393	32.7%

Table 1. Geometric registration evaluation on the KITTI (left) and Oxford RobotCar dataset (right) as evaluated by RANSAC. The proposed method performs commensurately to the state-of-the-art, while achieving a higher inlier rate and requiring fewer number of iterations.

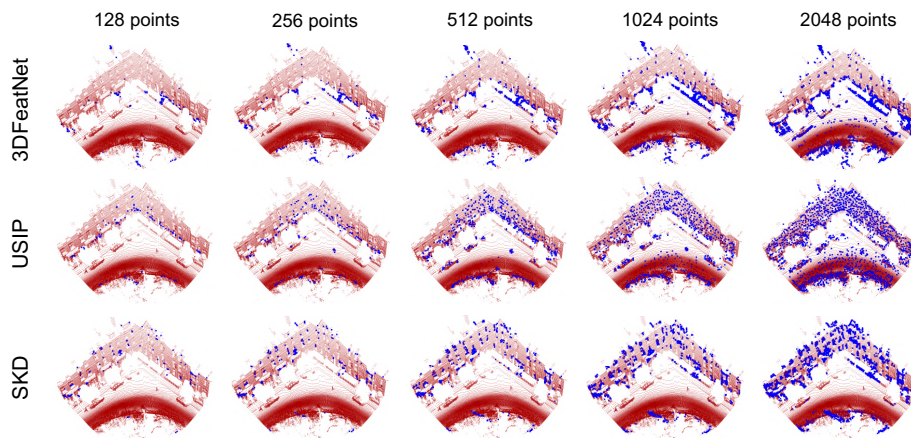


Fig. 8. Qualitative results on the Oxford RobotCar dataset.

Fig. 6 (right) illustrates the repeatability of our approach on the KITTI dataset. On this dataset, 3DFeatNet performs slightly better than on the Oxford RobotCar dataset. Interestingly, as we use the feature signal of 3DFeatNet, our keypoint detector also performs better. In addition, Fig. 7 presents qualitative evaluation of our approach on the KITTI dataset with increased number of keypoints, where SKD consistently selects the same areas of the environment.

4.6 Geometric Verification Experiments

We present the results of the geometric registration on the KITTI and Oxford RobotCar datasets in Tab. 1. SKD performs similarly to the state-of-the-art in terms of relative rotation and translation error - within the standard deviation of the best-performing method. Our method is, however, approximately nine times faster on the KITTI dataset and two times faster on the Oxford RobotCar dataset compared to the second-best approach. Furthermore, due to the high repeatability and matchability scores, SKD has the highest number of inliers.

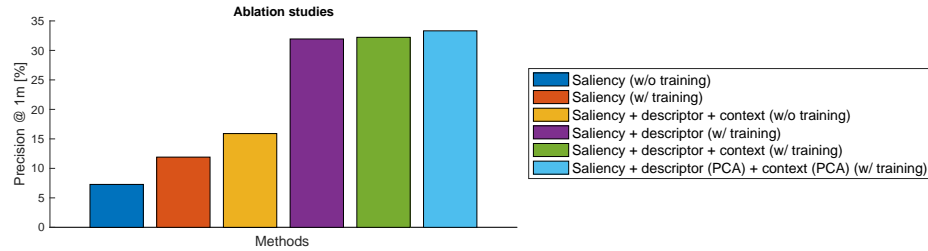


Fig. 9. Ablation studies of our method evaluated on the Oxford RobotCar dataset. We evaluate the contribution of the saliency information, and the importance of training with the original descriptor. The results displayed in the figure show the clear contribution the neural network is making to the keypoint generation process.

4.7 Ablation studies

In Fig. 9, we show the precision at 1 m distance on the Oxford RobotCar dataset while evaluating each of the components of our approach.

First, we inspected the contribution of the saliency in the concatenated vector. In our experiments the saliency information alone is responsible for approximately half of the concatenated vector - dark blue compared to yellow in Fig. 9. In addition, training a neural network with just saliency information contributes to approximately a third of the end result - red compared to light blue. For these reasons we have decided to name our method Saliency Keypoint Detector (**SKD**). Second, the sheer contribution of the network when training with the full feature vector is substantial as is to be expected - purple compared to dark blue and yellow on Fig. 9. Third, adding the context features and performing PCA on both the context and the descriptor features slightly increases the performance. Our intuition is that PCA smooths the learned feature space, which leads to better generalization.

5 Conclusions

In this paper we present a novel method for keypoint extraction that uses saliency information to extract informative regions in a point cloud. The method concatenates signals from the gradients with respect to the input, context-aware features and the descriptor features and learns to predict which 3D points have a higher chance of being matched correctly. The proposed approach is descriptor-agnostic and outperforms the state-of-the-art by up to 50% in matchability and repeatability compared to the second-best method. When performing geometric registration, the algorithm achieves a higher number of inliers while also finding a correct transformation significantly faster than the current state-of-the-art.

References

1. Adebayo, J., Gilmer, J., Muelly, M., Goodfellow, I., Hardt, M., Kim, B.: Sanity checks for saliency maps. In: *Advances in Neural Information Processing Systems* (2018)
2. Ancona, M., Ceolini, E., ztireli, C., Gross, M.: Towards better understanding of gradient-based attribution methods for deep neural networks. In: *International Conference on Learning Representations* (2018)
3. Baehrens, D., Schroeter, T., Harmeling, S., Kawanabe, M., Hansen, K., Müller, K.R.: How to explain individual classification decisions. *J. Mach. Learn. Res.* **11**, 1803–1831 (Aug 2010)
4. Benbihi, A., Geist, M., Pradalier, C.: ELF: embedded localisation of features in pre-trained CNN. In: *ICCV* (2019)
5. Deng, H., Birdal, T., Ilic, S.: Ppfnet: Global context aware local features for robust 3d point matching. In: *The IEEE Conference on Computer Vision and Pattern Recognition (CVPR)* (2018)
6. Fischler, M.A., Bolles, R.C.: Random sample consensus: A paradigm for model fitting with applications to image analysis and automated cartography. *Commun. ACM* **24**(6), 381–395 (1981)
7. Geiger, A., Lenz, P., Stiller, C., Urtasun, R.: Vision meets robotics: The KITTI dataset. *International Journal of Robotics Research* **32**(11), 1231 – 1237 (2013)
8. Georgakis, G., Karanam, S., Wu, Z., Ernst, J., Koeck, J.: End-to-end learning of keypoint detector and descriptor for pose invariant 3d matching. In: *CVPR* (2018)
9. Harris, C., Stephens, M.: A combined corner and edge detector. In: *Fourth Alvey Vision Conference* (1988)
10. Jakab, T., Gupta, A., Bilen, H., Vedaldi, A.: Unsupervised learning of object landmarks through conditional image generation. In: *Advances in Neural Information Processing Systems* (2018)
11. Kapur, J., Sahoo, P., Wong, A.: A new method for gray-level picture thresholding using the entropy of the histogram. *Computer Vision, Graphics, and Image Processing* **29**(3), 273 – 285 (1985)
12. Kulkarni, T., Gupta, A., Ionescu, C., Borgeaud, S., Reynolds, M., Zisserman, A., Mnih, V.: Unsupervised learning of object keypoints for perception and control. In: *Advances in Neural Information Processing Systems* (2019)
13. Li, J., Lee, G.H.: Usip: Unsupervised stable interest point detection from 3d point clouds. In: *ICCV* (2019)
14. Li, Y., Bu, R., Sun, M., Wu, W., Di, X., Chen, B.: Pointcnn: Convolution on x-transformed points. In: *NeurIPS, Advances in Neural Information Processing Systems* (2018)
15. Liu, Z., Tang, H., Lin, Y., Han, S.: Point-voxel CNN for efficient 3d deep learning. In: *Advances in Neural Information Processing Systems* (2019)
16. Lowe, D.G.: Distinctive image features from scale-invariant keypoints. *Int. J. Comput. Vision* (2004)
17. Lu, W., Wan, G., Zhou, Y., Fu, X., Yuan, P., Song, S.: DeepVCP: An end-to-end deep neural network for point cloud registration. In: *Proceedings of the IEEE International Conference on Computer Vision*. pp. 12–21 (2019)
18. Maddern, W., Pascoe, G., Linegar, C., Newman, P.: 1 Year, 1000km: The Oxford RobotCar Dataset. *The International Journal of Robotics Research (IJRR)* **36**(1), 3–15 (2017)

19. Mahendran, A., Vedaldi, A.: Salient deconvolutional networks. In: European Conference on Computer Vision (2016)
20. Mao, J., Wang, X., Li, H.: Interpolated convolutional networks for 3d point cloud understanding. In: The IEEE International Conference on Computer Vision (ICCV) (2019)
21. Qi, C.R., Liu, W., Wu, C., Su, H., Guibas, L.J.: Frustum pointnets for 3d object detection from rgb-d data. In: The IEEE Conference on Computer Vision and Pattern Recognition (CVPR) (2018)
22. Qi, C.R., Su, H., Mo, K., Guibas, L.J.: PointNet: Deep Learning on Point Sets for 3D Classification and Segmentation. In: IEEE Conference on Computer Vision and Pattern Recognition (CVPR) (2017)
23. Qi, C.R., Yi, L., Su, H., Guibas, L.J.: PointNet++: Deep Hierarchical Feature Learning on Point Sets in a Metric Space. In: NeurIPS, Advances in Neural Information Processing Systems (2017)
24. Ren, S., He, K., Girshick, R., Sun, J.: Faster r-cnn: Towards real-time object detection with region proposal networks. In: Advances in Neural Information Processing Systems 28 (2015)
25. Savinov, N., Seki, A., Ladicky, L., Sattler, T., Pollefeys, M.: Quad-networks: unsupervised learning to rank for interest point detection. In: CVPR (2017)
26. Selvaraju, R.R., Cogswell, M., Das, A., Vedantam, R., Parikh, D., Batra, D.: Grad-cam: Visual explanations from deep networks via gradient-based localization. In: 2017 IEEE International Conference on Computer Vision (ICCV) (2017)
27. Selvaraju, R.R., Cogswell, M., Das, A., Vedantam, R., Parikh, D., Batra, D.: Grad-cam: Visual explanations from deep networks via gradient-based localization. In: The IEEE International Conference on Computer Vision (ICCV) (Oct 2017)
28. Simonyan, K., Vedaldi, A., Zisserman, A.: Deep inside convolutional networks: Visualising image classification models and saliency maps. In: Workshop at International Conference on Learning Representations (2014)
29. Springenberg, J., Dosovitskiy, A., Brox, T., Riedmiller, M.: Striving for simplicity: The all convolutional net. In: Workshop at International Conference on Learning Representations (2015)
30. Uy, M.A., Lee, G.H.: PointNetVLAD: Deep Point Cloud Based Retrieval for Large-Scale Place Recognition. In: IEEE Conference on Computer Vision and Pattern Recognition (CVPR) (2018)
31. Verdie, Y., Yi, K.M., Fua, P., Lepetit, V.: TILDE: A temporally invariant learned detector. In: CVPR (2014)
32. Wang, Y., Solomon, J.M.: Deep Closest Point: Learning representations for point cloud registration. In: Proceedings of the IEEE International Conference on Computer Vision. pp. 3523–3532 (2019)
33. Xiang, C., Qi, C.R., Li, B.: Generating 3d adversarial point clouds. In: The IEEE Conference on Computer Vision and Pattern Recognition (CVPR) (June 2019)
34. Xu, D., Anguelov, D., Jain, A.: Pointfusion: Deep sensor fusion for 3d bounding box estimation. In: The IEEE Conference on Computer Vision and Pattern Recognition (CVPR) (2018)
35. Yew, Z.J., Lee, G.H.: 3dfeat-net: Weakly supervised local 3d features for point cloud registration. In: ECCV (2018)
36. Yi, K.M., Trulls, E., Lepetit, V., Fua, P.: Lift: Learned invariant feature transform. In: European Conference on Computer Vision (2016)
37. Zhang, W., Xiao, C.: PCAN: 3d attention map learning using contextual information for point cloud based retrieval. In: The IEEE Conference on Computer Vision and Pattern Recognition (CVPR) (2019)

38. Zhang, Y., Guo, Y., Jin, Y., Luo, Y., He, Z., Lee, H.: Unsupervised discovery of object landmarks as structural representations. In: IEEE Conference on Computer Vision and Pattern Recognition (CVPR) (2018)
39. Zheng, T., Chen, C., Yuan, J., Ren, K.: Pointcloud saliency maps. In: ICCV (2019)
40. Zhong, Y.: Intrinsic shape signatures: A shape descriptor for 3d object recognition. In: 2009 IEEE 12th International Conference on Computer Vision Workshops, ICCV Workshops. pp. 689–696. IEEE (2009)